Integral-equation approach to the surface structure of classical insulating liquids

R. A. McGough and M. D. Miller
Department of Physics, Washington State University, Pullman, Washington 99164-2814
(Received 21 February 1986)

We have obtained self-consistent solutions to the hypernetted-chain integral equation in a planar surface geometry. The surface density profiles are monotonic with a constant negative gradient and show no surface structure. We compute the surface total correlation function and direct correlation function and also report on the temperature dependence of the surface tension, the position of the Gibbs dividing surface, and the surface width.

I. INTRODUCTION

The structure of classical liquid surfaces and interfaces is an old and formidable problem of condensed matter physics.[1] Basic questions are still being raised concerning the existence and proper definitions of intrinsic surface profiles.[2–5] To date most information concerning the interfacial structure on a microscopic level has been obtained from molecular dynamics[6] or Monte Carlo[7] simulations. This situation should be contrasted with that of the uniform phases where complimentary perturbative, integral equation, and stochastic approaches have each been developed to give a deep and insightful picture of the microscopic structure. The need to develop methods to supplement the stochastic approaches is especially acute for nonuniform liquids. If one uses a small system in the simulation in order to better emphasize the surface then fluctuations can be large and one can question whether the information corresponds to a macroscopic surface. On the other hand, in a large system the surface energy is a small fraction of the total energy and so it is possible for the stochastic approaches to develop metastable surface structure. For a summary description of the various conclusions reached in simulations of the liquid-gas interface see Ref. 8.

An integral-equation approach does not suffer from this problem. One concentrates the computational effort on the surface region and whatever structure is found is due to the underlying equilibrium state. The drawback with integral-equation approaches is that they are approximate in the sense that various classes of cluster diagrams are omitted. Experience with the bulk, however, gives some confidence that integral-equation solutions can be fairly accurate representations of the exact stochastic results.[9] In this letter we wish to report the first self-consistent solutions of a set of integral equations which describe a fluid with a planar surface geometry.

II. THEORY

We consider a fluid with N particles in a volume Ω and seek to determine the n-body distribution functions, $\rho^{(n)}(1,2,\ldots,n)$, in the coexistence region. For a single-component system there is one independent thermodynamic field along the coexistence curve which we choose to be the temperature, T. We introduce an external symmetry breaking field $U_{\rm ext}=\sum_i u(z_i)$ into the Hamiltonian. Below the critical temperature, T_c, an interface will form in a plane normal to the z axis with the liquid phase in the lower half space. By definition,

$$\rho^{(n)}(1,2,\ldots,n)=\frac{N!}{(N-n)!}\frac{\int \exp[-\beta(U_{\rm ext}+\Phi)]d\mathbf{r}_{n+1}d\mathbf{r}_{n+2}\cdots d\mathbf{r}_N}{\int \exp[-\beta(U_{\rm ext}+\Phi)]d\mathbf{r}_1 d\mathbf{r}_2\cdots d\mathbf{r}_N}\ , \tag{1}$$

where $\beta=1/k_BT$ and Φ is the total interparticle potential. In particular, the surface density profile $\rho(z_1)\equiv\rho^{(1)}(1)$. We now introduce the total correlation function $h(1,2)$ where

$$h(1,2)=g(1,2)-1 \tag{2}$$

and $\rho^{(2)}(1,2)=\rho(1)\rho(2)g(1,2)$.

The total correlation function is in turn related to the two-particle direct correlation function by means of the Ornstein-Zernike (OZ) equation:

$$h(1,2)=c(1,2)+\int d3\,\rho(3)h(1,3)c(3,2)\ . \tag{3}$$

The role of the direct correlation function in the theory of nonuniform liquids has been discussed extensively.[10] If we take advantage of the translational invariance of our system in the XY plane, then the Ornstein-Zernike (OZ) equation can be written

$$h_\kappa(z_1,z_2)=c_\kappa(z_1,z_2)+\int_{-\infty}^{\infty}dz_3\,\rho(z_3)h_\kappa(z_1,z_3)c_\kappa(z_e,z_2)\ , \tag{4}$$

where $h_\kappa(z_1,z_2)$ is the Hankel transform of $h(1,2)$:

$$h_\kappa(z_1,z_2)=2\pi\int_0^\infty d\rho\,\rho J_0(\kappa\rho)c(\rho,z_1,z_2)\ , \tag{5}$$

and the $\{\kappa\}$ are surface wave vectors. Likewise, $c_\kappa(z_1,z_2)$ is the Hankel-transformed surface direct correlation func-

tion $c(1,2)$. (For the sake of clarity, we have suppressed the temperature in the arguments of the various functions.)

The surface distribution function, $g(1,2)$ and direct correlation function $c(1,2)$ are related by the hypernetted-chain (HNC) equation

$$g(1,2)=\exp[-\beta\phi(r_{12})+X(1,2)+E(1,2)] , \quad (6)$$

where $\phi(r)$ is the two-particle potential function and $X(1,2)=h(1,2)-c(1,2)$. We obtain the lowest-order HNC equation (HNC/0) by omitting the sum of the elementary diagrams; i.e., setting $E(1,2)=0$. Several methods for correcting this basic result have been developed and will be discussed below. A discussion of the application of this integral equation as applied to the uniform bulk phase, can be found in Ref. 9.

In order to close the set of equations, we need a relation to determine $\rho(z)$. There are several possibilities.[1] The most popular choice has been the first Born-Bogoliubov-Green-Kirkwood-Yvon (BBGKY) equation.[1] We have found, however, that an alternative form using the one-particle direct correlation function $c^{(1)}(1)$ is easier to implement. Thus we use

$$\rho(z)=(z_0/\lambda_T{}^3)\exp[-\beta u(z)+c(z)] , \quad (7)$$

where z_0 is the activity, λ_T is the thermal de Broglie wavelength, and with no ambiguity, we can drop the superscript 1 on $c(z)$. The one-particle direct correlation function (DCF) is the generator of the higher DCF's, in particular, $\delta c(1)/\delta\rho(2)=c(1,2)$, an immediate consequence of which is

$$\nabla_1 c(1)=\int d2\, c(1,2)\nabla_2\rho(2) . \quad (8)$$

Equations (5)—(8) then form a closed set of relations for the functions $\rho(1)$, $c(1)$, $g(1,2)$, and $c(1,2)$ for a given T, $\phi(r)$, and $u(z)$.

We have chosen the two-particle potential to be in Lennard-Jones (LJ) form, $\phi(r)=4(r^{12}-r^{-6})$ (which defines the usual reduced units). The LJ potential is a reasonable representation of the interaction in a simple insulating liquid. Its extensive previous use allows it to serve as a reference system to compare results from various approaches. The particular form used for the external field is irrelevant as will be discussed below.

III. DISCUSSION

We shall begin with a brief sketch of the numerical work. We divide the z axis into three regions: one in the bulk liquid, one in the bulk vapor, and the third which encompasses the interface (we shall call this central region the calculational window). The portion of the z axis in the calculational window is discretized onto a set of N points. Then if we use N_κ surface wave vectors, the surface OZ equation becomes $N\times N_\kappa$ linear equations. Typically this means 1000—2000 equations. These equations were solved by standard numerical methods.[11] The OZ equation together with Eqs. (6)—(8) were then solved simultaneously by a Picard-like iterative scheme. There are numerous numerical parameters which must be set carefully in order to ensure accurate results. The list of these parameters includes the ρ, κ, and z grid sizes and the maximum values used for ρ and κ. The great bulk of the numerical work is contained in computing Hankel and inverse Hankel transforms accurately and in solving the large set of linear equations. These aspects are not strongly dependent on the density function and so they can be tested in the uniform limit where highly accurate bulk algorithms are available. In the work reported below, we used 25 values of ρ and κ and 49 values of z. In the following we shall discuss the results of this calculation, further details of the numerical work will be published elsewhere.

In Fig. 1 we show surface density profiles for a range of temperatures $\lesssim T_c$. We find by inspection that $T_c\approx 1.26$ and $\rho_c\approx 0.35$. We note that this represents an *independent* determination of the HNC critical point. These numbers can be compared with those determined by analyzing bulk equations of state.[12] We find that our results are in strong disagreement with critical constants obtained by analyzing the compressibility ($T_c\approx 1.39$ and $\rho_c\approx 0.28$). Better agreement is obtained, however, with those critical constants obtained by employing virial theorem ρ_c (~ 0.26). The shape of our surface profiles have a monotonic negative gradient with *no* evidence for any enhanced surface structure.

The results shown in Fig. 1 are for a fixed normalization (that is, a fixed number of particles per unit area in the calculational window). The results are independent of the value of the normalization. Changing the normalization rigidly translates the surface through the calculational window. This effect is shown explicitly in the inset of Fig. 1 for the $T=1.1$ surface profile. In Table I, we have collected various results including the estimated bulk

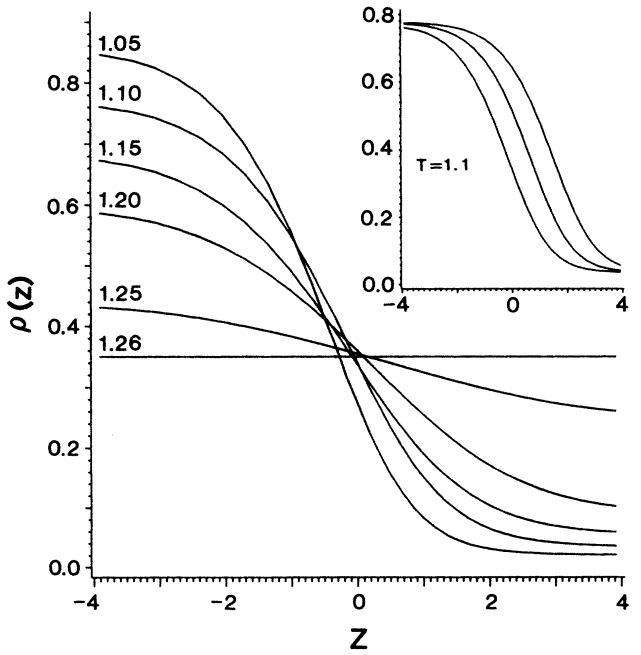

FIG. 1. HNC surface density profiles for $T=1.050$, 1.10, 1.15, 1.20, 1.25, and 1.26. The inset shows the $T=1.1$ surface profile as a function of normalization.

liquid and vapor densities, the position of the Gibbs dividing surface and the surface width. The results at the highest temperature are clearly suspect since the surface width is nearly the size of the calculational window. (The width reported in Table I is the conventional 90-10 extent.[13])

The temperature dependence of z_G, the position of the Gibbs dividing surface (the surface of zero excess number density), is interesting. As T increases towards T_c, z_G moves outward from the liquid into the vapor half-space. This implies a skewed density profile quite distinct from a simple mean-field tanh-like form but in qualitative agreement with a somewhat more realistic penetrable sphere model.[14] It should be stressed that the density profiles used in the analysis were obtained for a fixed number of particles per unit area in the calculational window.

In Fig. 2 we show the surface total correlation function $h(\rho,z,z)$ at $T=1.10$ taking slices parallel to the interface. The bulk liquid and gas phase $h(r)$'s differ mainly in the presence or absence, respectively, of structure following the nearest-neighbor peak. The remarkable aspect of this figure is the apparent *enhancement* of the nearest-neighbor peak in the region of the interface. We note, however, that this is probably the effect of too coarse a ρ grid.

In Figs. 3 and 4 we show parallel slices of the structure functions $h_\kappa(z,z)$ and $c_\kappa(z,z)$ at $T=1.10$. (The z axes have been reversed relative to Fig. 1.) The strong short-ranged repulsion in the Lennard-Jones potential is reflected in the long-ranged κ dependence of the structure functions. In Fig. 5, we show a transverse slice of $c_\kappa(z_1,z_2)$ with $\kappa=0.687$, a small wave vector. In this view, the correlations contained in $c_\kappa(z_1,z_2)$ have died out for $|z_{12}|>2$.

There are two fundamental approaches to computing the surface tension, σ, which can be shown to be formally equivalent.[15] The Kirkwood-Buff (KB) expression can be obtained by considering the functional derivative of the grand potential with respect to the pair potential.[1] One finds

$$\sigma=\tfrac{1}{4}\int_{-\infty}^{\infty} dz_1\,\rho(z_1)\int d2\,\rho(z_2)(r_{12}-3z_{12}^2/r_{12}) \times\phi'(r_{12})g^{(1,2)}\,. \tag{9}$$

This expression is difficult to implement numerically because the strong short-ranged repulsion in $\phi(r)$ requires a dense grid for $g(\rho_{12},z_1,z_2)$. The spacing which we used in this calculation is simply too large (cf. Fig. 2). There is an alternative expression, however, which uses the DCF and, for smooth density profiles, is much simpler than KB:

$$\sigma=(T/4)\int_{-\infty}^{\infty} dz_1\,\rho'(z_1)\int d2\,\rho'(z_2)(x_2^2+y_2^2)c(1,2)\,, \tag{10}$$

where primes denote differentiation. In Fig. 6 and Table I we show the results from Eq. (5). The surface tension clearly vanishes in the region $T\approx 1.26$. The inverted triangle is a Monte Carlo result from Ref. 7. The good

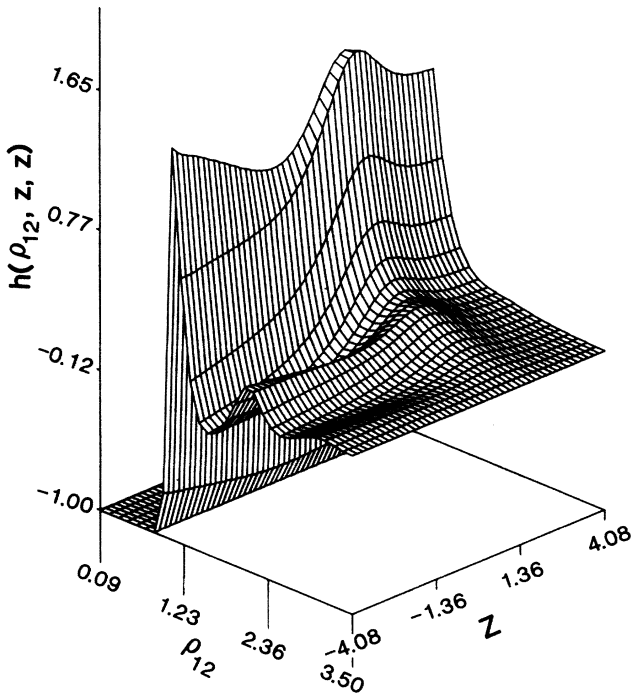

FIG. 2. The total correlation function $h(\rho_{12},z,z)$ for $T=1.1$. We note the enhanced nearest-neighbor peak in the interfacial region.

TABLE I. HNC liquid-gas coexistence curve: ρ_l and ρ_v are the estimated bulk phase densities, z_G is the position of the Gibbs dividing surface, h is the 90-10 surface width, and σ is the surface tension.

T	ρ_l	ρ_v	z_G	h	σ
1.050	0.85	0.020	−0.64	3.1	0.68
1.075	0.81	0.027	−0.49	3.3	0.57
1.100	0.77	0.035	−0.33	3.6	0.48
1.125	0.72	0.044	−0.38	3.8	0.39
1.150	0.68	0.057	−0.22	4.1	0.31
1.175	0.64	0.074	−0.06	4.4	0.24
1.200	0.59	0.100	0.09	4.7	0.17
1.225	0.54	0.140	0.23	5.1	0.11
1.250	0.44	0.250	0.23	6.2	0.02

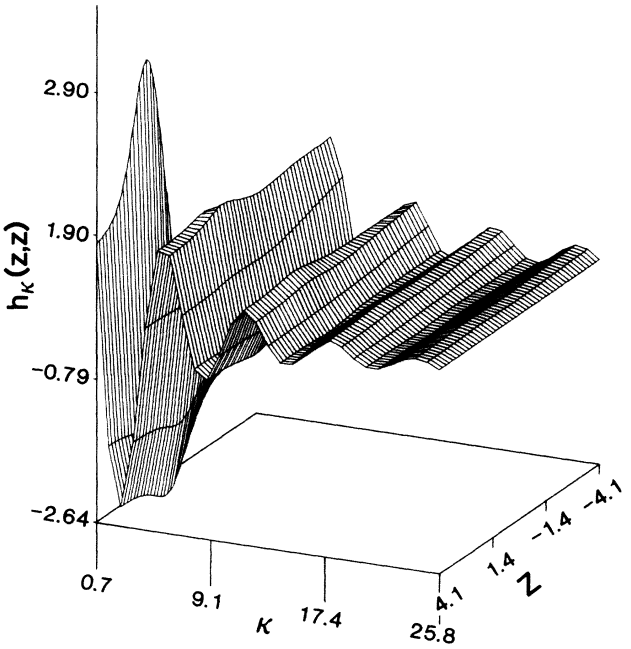

FIG. 3. The surface structure function $h_\kappa(z,z)$ at $T=1.1$. The long-range correlations in the interfacial region can be seen as enhanced small-κ structure.

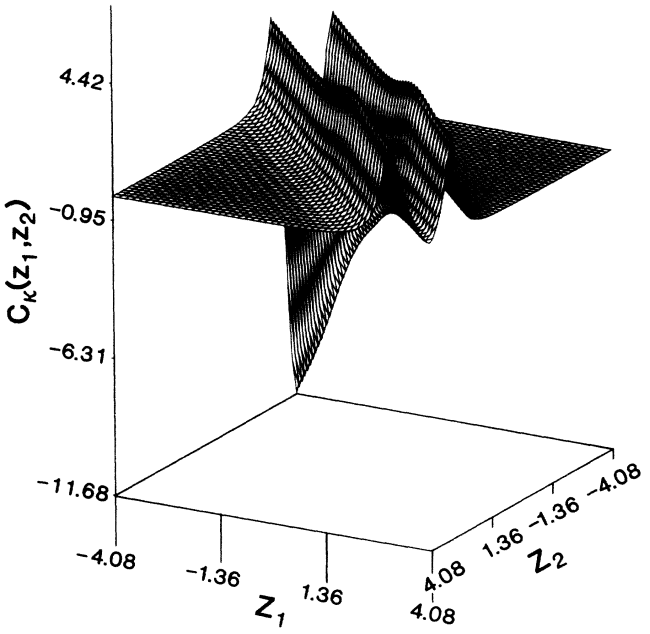

FIG. 5. The Hankel-transformed direct correlation function $c_\kappa(z_1,z_2)$ at $T=1.1$ in a transverse view, $\kappa=0.687$.

agreement with the HNC surface tension is probably fortuitous.

We note in passing that the long-ranged correlations in the interfacial region for the surface structure function, $h_\kappa(z,z)$, as discussed by Wertheim[16] can be vividly seen as the enhanced small-κ behavior in Fig. 3 (see also Ref. 6).

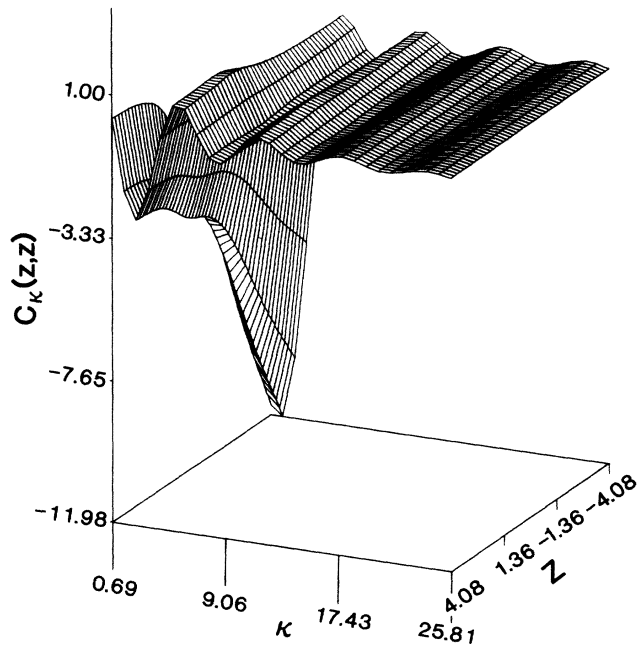

FIG. 4. The Hankel-transformed direct correlation function $c_\kappa(z,z)$ at $T=1.1$.

IV. CONCLUSION

In this paper we have reported one- and two-particle surface structure functions which have been calculated as solutions of a set of integral equations. *No ad hoc* assumptions have been made concerning the form of the two-particle distribution function (e.g., a local density approximation). For $T > T_c$, our approach yields bulk radial distribution functions and DCF's which are in excellent agreement with those computed with a high-precision bulk algorithm.[17] We found that for $T < T_c$, an initial input of a nonuniform density profile was sufficient to nu-

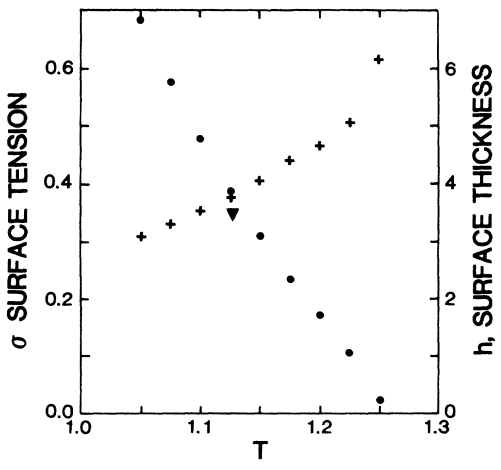

FIG. 6. The surface tension σ and surface interface width h as functions of temperature. The △ is a Monte Carlo data point from Ref. 7.

cleate a surface (i.e., the results presented above were obtained in *zero* external field). The final profiles were checked to ensure that they were independent of the particular initial configuration.

We point out that a related system, a liquid in contact with a solid surface, has received detailed treatment by integral equation techniques.[18]

Capillary wave theory predicts that the surface width should have a nontrivial $(\ln A)^{1/2}$ dependence where A is the surface area. This weak divergence should apply to the surfaces we considered since these surfaces are all determined in zero external field. We are thus led to consider the question: Why have we obtained well-defined surfaces? There are several possible answers. First, the HNC/0 approximation might not include the long-wavelength capillary modes. However, as pointed out above, Fig. 3 clearly shows enhanced long-ranged correlations in the interfacial region. Second, this effect was somehow lost in the numerical work. We carefully checked the parameters used for the computations and did not find that the surface thickened with smaller grid sizes, longer cutoffs for the integrals, or a larger calculational window. Third, and most probable, is the fixed normalization. We found that we could only achieve stable convergence of the iterative scheme by fixing the number of particles per unit area in the calculational window. This procedure seems to project out one particular surface from the infinite number of equivalent surfaces obtainable by rigid translations along the z axis. Thus, in this sense, one may speculate that our solutions might be related to the intrinsic profiles as discussed by Evans.[3]

In further work, we shall report on a similar study using the Percus-Yevick (PY) equation. The thermodynamic inconsistencies of the HNC and PY equations result in coexisting liquid and vapor phases which are at different bulk virial pressures. (This is the reason why the critical constants reported here differ from those analyzed from bulk equations of state.) It is possible, however, to devise a tractable algorithm for the surface problem which generalizes the enforced thermodynamic consistency methods[19,20] used for the bulk. This work will also be reported elsewhere. We shall also report on a spectral analysis of the functions

$$C_\kappa(z_1,z_2)=\delta(z_1-z_2)/\rho(z_1)-c_\kappa(z_1,z_2)$$

and

$$H_\kappa(z_1,z_2)=\delta(z_1-z_2)+\rho(z_1)\rho(z_2)h_\kappa(z_1,z_2)$$

which, following Wertheim's analysis,[14] yield important information on the onset of long-ranged correlations in the interfacial region.

We noted above that Eqs. (9) and (10) were formally equivalent expressions for the surface tension. However, they may not yield identical results when using distribution functions and direct correlation functions which are solutions of an approximate integral equation. This point will be addressed by obtaining solutions with much smaller grid sizes which will enable us to obtain accurate results from the Kirkwood-Buff expression.

ACKNOWLEDGMENT

This investigation was supported in part by funds provided by the Washington State University Research and Arts Committee. We also acknowledge the support of the Washington State University Computing Service Center.

[1]For a recent survey of the field, see J. S. Rowlinson and B. Widom, *Molecular Theory of Capillarity* (Oxford, London, 1982).

[2]J. D. Weeks, J. Chem. Phys. **67**, 3106 (1977); Phys. Rev. Lett. **52**, 2160 (1984); D. A. Huse, W. van Saarloos, and J. D. Weeks, Phys. Rev. B **32**, 233 (1985).

[3]R. Evans, Mol. Phys. **42**, 1169 (1981).

[4]B. Widom, in *Phase Transitions and Critical Phenomena*, edited by C. Domb and M. S. Green (Academic, New York, 1972), Vol. 2.

[5]G. Chapela, G. Savile, S. M. Thompson, and J. S. Rowlinson, Ref. 7, Chap. 4, and references therein.

[6]M. H. Kalos, J. K. Percus, and M. Rao, J. Stat. Phys. **17**, 111 (1977).

[7]G. Chapela, G. Savile, S. M. Thompson, and J. S. Rowlinson, J. Chem. Soc. Faraday Trans. II **73**, 1133 (1977).

[8]J. P. Valleau and G. M. Torrie, in *Statistical Mechanics Part A: Equilibrium Techniques*, edited by B. J. Berne (Plenum, New York, 1977).

[9]See, e.g., J. P. Hansen and I. R. McDonald, *Theory of Simple Liquids* (Academic, New York, 1976).

[10]For a detailed discussion, see J. K. Precus, in *The Liquid State of Matter: Fluids Simple and Complex*, edited by E. W. Montroll and J. L. Lebowitz (North-Holland, Amsterdam, 1982), and references cited therein.

[11]J. J. Dongarra, C. B. Moler, J. R. Bunch, and G. W. Stewart, *Linpack Users' Guide* (SIAM, Philadelphia, 1979).

[12]For a compilation of various authors' HNC (and PY) critical points, see D. Levesque, Physica **3**, 1985 (1966).

[13]J. S. Rowlinson and B. Widom, Ref. 1, p. 180.

[14]J. S. Rowlinson and B. Widom, Ref. 1, p. 157.

[15]J. S. Rowlinson and B. Widom, Ref. 1, pp. 104–109.

[16]M. S. Wertheim, J. Chem. Phys. **65**, 2377 (1976).

[17]M. D. Miller, Phys. Rev. B **14**, 3937 (1976).

[18]R. M. Nieminen and N. W. Ashcroft, Phys. Rev. A **24**, 560 (1981); S. M. Foiles and N. W. Ashcroft, Phys. Rev. B **25**, 1366 (1982); K. Hillebrand and R. M. Nieminen, Surf. Sci. **147**, 599 (1984); and references cited therein.

[19]F. J. Rogers and D. A. Young, Phys. Rev. A **30**, 999 (1984).

[20]F. Lado, J. Chem. Phys. **81**, 4592 (1984).

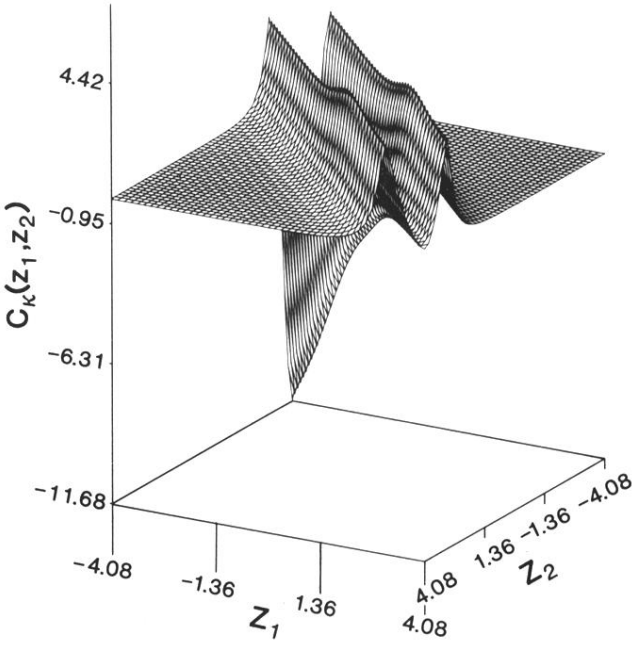

FIG. 5. The Hankel-transformed direct correlation function $c_\kappa(z_1,z_2)$ at $T=1.1$ in a transverse view, $\kappa=0.687$.